

Kinesin motion in the absence of external forces characterized by interference total internal reflection microscopy

Giovanni Cappello,* Mathilde Badoual, Albrecht Ott, and Jacques Prost
Physico Chimie Curie, UMR CNRS/IC 168, 26 rue d'Ulm, 75248 Paris Cedex 05, France

Lorenzo Busoni
Physico Chimie Curie, UMR CNRS/IC 168, 26 rue d'Ulm, 75248 Paris Cedex 05, France
and Department of Physics, University of Florence and INFN, Via G. Sansone 1, 50019 Sesto Fiorentino, Firenze, Italy
 (Received 14 February 2002; revised manuscript received 15 April 2003; published 15 August 2003)

We study the motion of the kinesin molecular motor along microtubules using *interference total internal reflection microscopy*. This technique achieves nanometer scale resolution together with a fast time response. We describe the first *in vitro* observation of kinesin stepping at high ATP concentration in the absence of an external load, where the 8-nm step can be clearly distinguished. The short-time resolution allows us to measure the time constant related to the relative motion of the bead-motor connection; we deduce the associated bead-motor elastic modulus.

DOI: 10.1103/PhysRevE.68.021907

PACS number(s): 87.15.-v, 87.80.-y, 07.79.Fc

I. INTRODUCTION

Many beautiful techniques which allow *in vitro* studies of single biological molecules such as DNA, RNA, and proteins have been developed over the past ten years. These techniques often involve observing mesoscopic objects such as beads or nanoneedles, to which the biomolecules are grafted. Current nanomanipulation techniques (i.e., atomic force microscopy, micropipettes, optical and magnetic tweezers) allow single molecules to be localized with nanometer precision and manipulated with forces down to a piconewton [1–4]. Using these techniques, several studies have been successfully conducted on biological machines, such as molecular motors and enzymes. However, the simultaneous control of force and position requires one to conjugate the molecule to a micrometer sized bead, which limits the time resolution of the experiments to the millisecond range. If a small bead (bead radius = 100 nm) is used, the bandwidth can be significantly improved [5,6].

We describe an evanescent wave microscopy technique for imaging small particles with high spatial and temporal resolutions. This method is based on the detection of light scattered from a single particle (i.e., bead) moving through an interference pattern generated by two identical laser beams undergoing total internal reflection at the glass/water interface. Measuring the temporal variations of the total scattered light allows us to estimate the position of an object moving in the fringes. In our experimental setup, we can reach a spatial resolution of a few nanometers ($\sim 1\%$ of fringe periodicity). Time resolution can be excellent (\sim microseconds) using a fast detector, such as a photomultiplier tube, but it is limited by the detector rise time and photon flux. Using this technique to observe molecular motor movement allows us to work in the absence of any external force. Moreover, we can measure the velocity, randomness,

kinesin step length, bead-motor elastic modulus, and the bead friction coefficient in a single experiment.

The experiments described in this paper are performed on kinesin with a very small cargo (50-nm bead) and without any external load. The kinesin microtubule is a protein complex, which catalyzes ATP hydrolysis: $\text{ATP} \Rightarrow \text{ADP} + \text{P}_i$. During the enzymatic reaction, the kinesin-microtubule complex converts chemical energy into mechanical work. Together with dynein-microtubule and myosin-actin complexes, it is responsible for intracellular transport, mitosis, and many other biological processes. Kinesin is a dimer of two identical subunits; it contains two motor heads and a coiled-coil tail. This two-headed motor moves processively [7] along microtubules towards the plus end, and travels over a mean distance of more than $1 \mu\text{m}$ without releasing from the microtubule. The fastest kinesins (*Neurospora Crassa* [8,9]) can reach speeds up to $2\text{--}3 \mu\text{m s}^{-1}$. Optical tweezers experiments have shown that kinesin develops a force of a few piconewtons (stall force $\approx 6\text{--}7$ pN) and that the motion is achieved by discrete steps of 8 nm [1,10]. This distance corresponds to the periodicity of the $\alpha\beta$ -tubulin arrangement in microtubules. Each step requires the hydrolysis of one-ATP molecule [11].

II. EXPERIMENTAL SETUP

A. Interference total internal reflection microscopy

As discussed previously, we localize the kinesin-coated bead with a precision of a few nanometers, in the microsecond range, by using a spatially modulated light [12]. This technique bears some similarity to earlier ones designed to study the proximal hydrodynamic behavior of polymers close to a surface [13]. A sinusoidal light modulation is obtained by interference of two laser beams, with opposite wave vector \vec{k}_x (the x direction being parallel to the microtubule long axis), with a fringe periodicity of

$$d = \frac{\lambda_0}{2n_{\text{glass}} \cos \theta},$$

*Electronic address: Giovanni.Cappello@Curie.fr

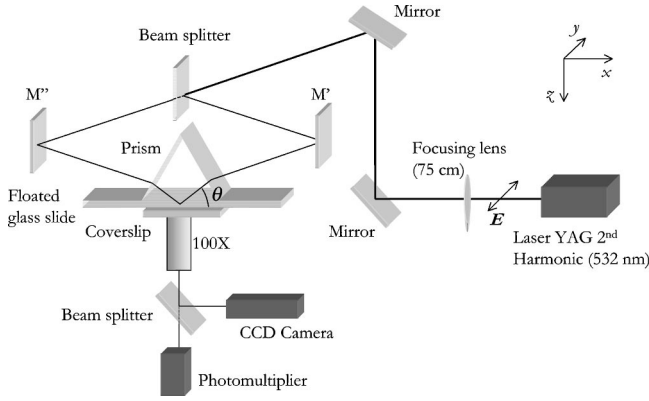


FIG. 1. Schematic of the experimental setup. The prism is required for total internal reflection.

where λ_0 is the laser wavelength, θ is the incidence angle at the glass/water interface (Fig. 1), and n_{glass} is the glass refraction index. As the bead scatters the light proportionally to the local electromagnetic field, its position $x(t)$ can be expressed as a function of the scattered intensity:

$$x(t) = \frac{d}{2\pi} \sin^{-1} \left[\frac{I(t) - (I_{max} + I_{min})/2}{(I_{max} - I_{min})/2} \right]. \quad (1)$$

The laser source wavelength currently used in the experiments is 532 nm, which implies that, with $n_{glass} = 1.518$, the fringe periodicity can be tuned down to 178 nm by changing the incidence angle θ . In our experiments, a typical value of θ is $24^\circ \pm 3^\circ$, corresponding to an interference periodicity of 192 ± 5 nm. This period can be experimentally measured by fixing a subwavelength single colloid on the slide and moving the sample holder by means of a calibrated piezoelectric stage. The measured mean value agrees with the expected one to within 4% (Fig. 2). The two beams, identical in divergence ($< 0.2^\circ$), intensity, phase, and polarization, are obtained using a flat beam splitter. The split beams are reflected on the sample, respectively, by mirrors M' and M'' . In order to obtain fringes with a well defined wave vector (direction x in the following), we set the same incidence angle θ for both the beams, with a precision greater than 0.5° .

If we take into account the laser polarization, the local intensity of the electric field at $z=0$ can be written as

$$I(x) \propto E^2 + [E_y^2 + E_{xz}^2 (\cos^2 \theta - \sin^2 \theta)] \sin\left(\frac{2\pi}{d}x\right),$$

where E_{xz} and E_y are, respectively, the components of the electric field perpendicular (P polarized) and parallel (S polarized) to the glass/water interface. We note from this equation that the fringe contrast,

$$C = \frac{E_y^2 + E_{xz}^2 (\cos^2 \theta - \sin^2 \theta)}{E^2},$$

has a maximum when the polarization vector is along the y axis ($E_{xz}=0$). In order to maximize the contrast, the laser polarization is set parallel to the glass/water interface.

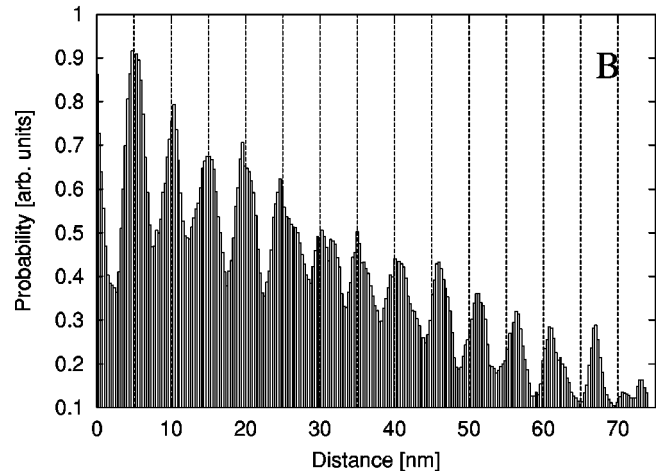
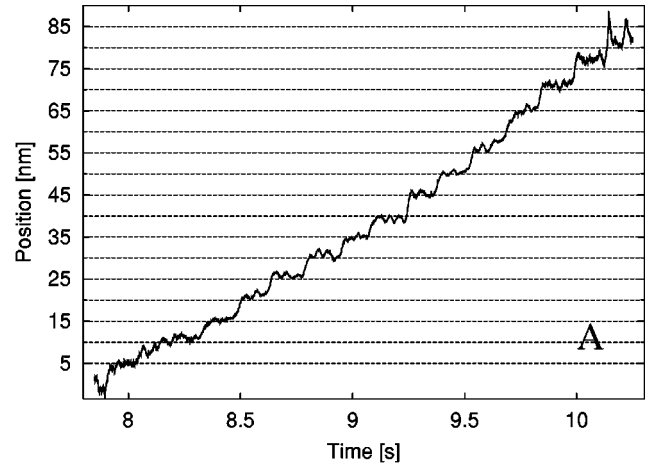


FIG. 2. Fringe calibration: a single colloid (diameter 40 nm) is fixed on the slide. The sample holder is moved in 5-nm steps by means of a calibrated piezoelectric stage. (a) The position of the bead is calculated from its luminosity according to Eq. (1). (b) Histogram of pairwise distances calculated from curve (a).

The resolution of this setup has been calibrated using a piezoelectric stage, which moves a bead stuck to the cover glass. Figure 2 shows the signal from a 40-nm bead, moving through the fringes in 5-nm steps. We observe that the measurements are accurate to within 2 nm. Eventually, we also verified that the drift of the pattern does not exceed 5–10 nm/s. This value is small enough to allow for the measurement of single-step events with ATP concentrations greater than $50 \mu M$. At this concentration, the uncertainty in the average velocity is smaller than 8% (3% in most cases). These figures could be improved, if necessary. With a 50-nm bead and our experimental conditions, one can expect to collect at most $\approx 10^9$ photons s^{-1} per bead [14,15]. Experimentally, we measure up to 10^8 photons s^{-1} per bead. We choose to work at grazing incidence in order to reduce the scattering volume, in which we collect only the intensity scattered from the beads near the interface (location of the microtubules). The penetration depth ζ can be tuned by adjusting the incidence angle. In our experiments, ζ is usually set to 100 ± 20 nm. The decay length of the evanescent field is measured by observing the optical signal due to the Brownian

motion of free beads in and out of the scattering volume. The same experiment provides an independent measurement of the bead diffusion constant, as discussed in Sec. III B.

The laser beam is focused on the sample slide over $\sim 100 \times 100 \mu\text{m}^2$. Since the laser beam waist is much larger than the distance between fringes ($\sim 200 \text{ nm}$), we approximate the intensity $I(x, z)$ as

$$I(x, z) = I_0 [1 + \sin(qx)] e^{-z/\xi}, \quad (2)$$

where z is the direction orthogonal to the glass surface, the origin is chosen at the interface, and $q = 2\pi/d$.

The external load due to the optical force can be deduced from Eq. (2) and the laser power. For a 1-W laser and a 50-nm-radius bead, the force is estimated to be 1000 times smaller than that which is exerted by optical tweezers. In our experimental setup, the “trapping” energy associated with the intensity gradient is $10^{-3} k_B T$, which is clearly negligible compared to the energy from Brownian motion.

Experiments are carried out using an inverted Zeiss Axiovert 100 microscope, equipped with an oil 100X DIC Plan Apochromat objective and a charge-couple device (CCD) camera. The laser source is a second-harmonic YAG (Coherent Verdi), with a wavelength $\lambda_0 = 532 \text{ nm}$ and a longitudinal coherence length of several hundreds meters. Its power is typically set to 400 mW. The scattered intensity is measured by a photomultiplier tube (Thorn-Emi 9125B) with a bandwidth of 100 kHz. Data are acquired using an analog-digital converter (Keithley instruments), with a sample rate up to 300 kHz. Any constant background is electronically subtracted by rejection of the DC component.

B. Bead assays

Bead assays are made with a biotinilated kinesin from *Drosophila*: HAtag KinBio401. The biotinilated HA-kinesin is purified from transformed *E. Coli* as described in Refs. [16,17]. Kinesin is then conjugated with streptavidin-coated latex beads ($r = 50 \pm 10 \text{ nm}$, Bangs laboratories). Beads are incubated for a few minutes in ultrasound bath with 5-mg/ml casein. This procedure prevents the beads from clustering.

Microtubules are assembled by polymerization of tubulin purified from pig brain and they are stabilized with 10- μM Taxol.

The flow chambers are built with a cover slip and a float glass microscope slide, spaced by two thin layers ($\sim 30 \mu\text{m}$) of vacuum grease. Microtubules stick to a poly-*L*-lysine coated slide. Microtubules are injected into the chamber and incubated for a few minutes. The chamber is then rinsed with BRB80 buffer (80-mM *K*-pipes, 1-mM MgCl_2 , 1-mM EGTA, pH 6.8) and flushed with a 5-mg/ml casein solution, in order to avoid nonspecific interactions between the beads and poly-*L*-lysine. The chamber is rinsed again and the kinesin-coated beads are injected into the chamber, together with the motility buffer (BRB80, 1-mM ATP, 1-mM GTP, and 10- μM Taxol).

After injection of kinesin-coated beads into the chamber, the beads randomly come into contact with the microtubules. Preliminary observations are performed by DIC microscopy. At room temperature, the kinesins move at $340 \pm 40 \text{ nm/s}$.

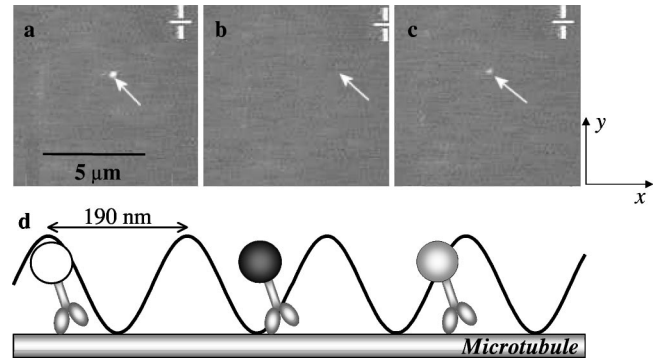


FIG. 3. (a)–(c) A kinesin-coated bead blinks moving through interference fringes in the near field. (d) Schematic view of the relationship between bead brilliance and its position.

This speed is appreciably slower than the velocities reported for analogous constructions [18,19]. However, many experiments have confirmed that the speed of this construction strongly depends on the buffer and on its pH [20].

In order to observe a single motor, the kinesin/bead ratio has been decreased to slightly above the limit where no beads move processively. Nevertheless, it is impossible to exclude the possibility that several motors interact simultaneously with the microtubules.

III. RESULTS

A. Kinesin steps

Bead motion is recorded by a CCD camera (25 frames/s) while the light intensity is measured by the photomultiplier tube. Figure 3 shows a kinesin-coated bead moving along the microtubule, from the left to the right, through the interference pattern (white arrows point toward the bead). We observe a strong variation of the scattered light when the bead moves from an antinode [Fig. 3(a)] to a node [Fig. 3(b)]. In Fig. 3(c), the bead is localized between these two positions. Figure 3(d) illustrates in which way the bead position can be determined from its brightness.

Figure 3(a) also shows that no photons are scattered by the microtubule itself, even if it is 30 nm thick (and therefore

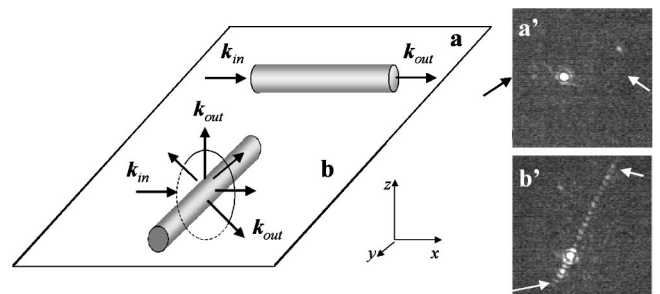


FIG. 4. (a) Scattering from a microtubule parallel to the wave vector \vec{k}_{in} : the momentum transfer is zero and $\vec{k}_{out} = \vec{k}_{in}$. (a') The two arrows point towards the end of the microtubule, which is invisible in this geometry. (b) and (b') Scattering from a microtubule perpendicular to the wave vector: the scattered beam must satisfy $|\vec{k}_{out}| = |\vec{k}_{in}|$ and \vec{k}_{out} perpendicular to the microtubule axis.

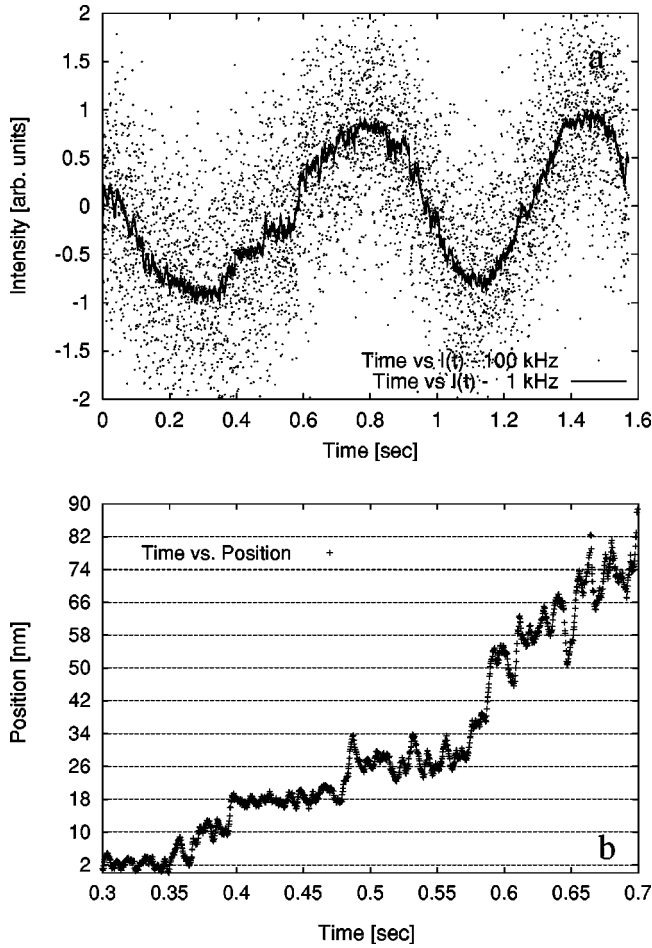


FIG. 5. Measured intensity as a function of time. (a) Data recorded with a bandwidth of 100 kHz (dots) and with a low-pass filter at 1 kHz (black line). Notice discontinuities in intensity variations. (b) Bead position calculated from curve *a* according to Eq. (1). The mean velocity of the motor is 340 ± 40 nm/s [19] at room temperature and 1-mM ATP. We choose a section of the curve with long plateaus.

not much smaller than the bead). In fact, we observe scattering from the microtubules only when their axis is perpendicular to the incident beam \vec{k}_{in} . This effect has a simple geometrical reason: the microtubule is much longer (1–10 μm) than the wavelength while its radius is 20 times smaller than the wavelength. Therefore, there is no momentum transfer along the microtubule axis [Fig. 4(a)] in the experimental geometry, and no light is transmitted through the objective. On the contrary, the light can be scattered if the incident wave vector is perpendicular to the microtubule [Fig. 4(b)].

The total scattered light collected by the photomultiplier tube is plotted in Fig. 5(a) as a function of time. The dots represent $I(t)$, acquired with a bandwidth of 100 kHz. Notice the low signal/noise ratio: *rms* noise is 33% of the average peak-to-peak signal modulation. This noise is essentially due to the Brownian motion of the bead and to the shot noise. In order to improve the signal/noise ratio, the signal is averaged by convolution with a box function. The continuous black line in Fig. 5(a) corresponds to the smoothed sig-

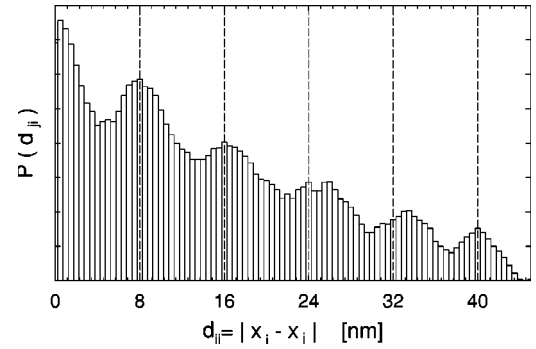


FIG. 6. Histogram of pairwise distances $d_{ij} = |x_i - x_j|$ for $i \neq j$, calculated from curve in Fig. 5(a) over four half periods.

nal, where the cutoff frequency of this low-pass filter is set to 1 kHz. The bead position $x(t)$ is calculated according to Eq. (1) over intervals of half a period. The *position vs time* function (black line) presents sudden jumps with discrete *steps* and *plateaus* in between. The discontinuities can be interpreted as the single steps of the kinesin, where the plateaus are the waiting time between two ATP hydrolysis events [1]. These steps have been statistically analyzed from several series of data. For each pair of points, $x(t_i)$ and $x(t_j)$, we calculate the distance $d_{ij} = |x(t_i) - x(t_j)|$, with $i \neq j$. The histogram of pairwise distances d_{ij} is plotted in Fig. 6. The histogram shows peaks around 8, 16, 25, 33, and 41 nm, which suggests a kinesin step of 8.2 ± 0.5 nm. This length is consistent with the periodicity of the microtubule and it reproduces, in the absence of external forces, the results obtained using optical tweezers. The histogram for a fixed bead moved by the mean of a calibrated piezoelectric stage does not exhibit any peak at all. This is to our knowledge the first observation of steps at high ATP concentration (1 mM), and without external forces.

B. Autocorrelation analysis

The $I(t)$ signal is extremely noisy when acquired with a bandwidth of 100 kHz (dots in Fig. 5). Two main sources of noise have been identified: the Brownian motion of the bead around the motor position and the shot noise. For a single bead, we collect up to 10^8 photons/s per bead, over a background of 5×10^8 photons/s, whereupon the shot noise is $\approx 14\%$ of the bead signal for a sample time of 3 μs . Both of these noises can be reduced by decreasing the bandwidth. The main disadvantage of this solution is that it simultaneously reduces the time resolution. However, the shot noise is uncorrelated, and computing the *intensity-intensity autocorrelation function* removes the shot noise while retains the useful information. With this procedure, the average over long acquisitions preserves the time resolution.

The autocorrelation function is defined as

$$\phi(\tau_j) = \frac{\langle I(t_i)I(t_{i+j}) \rangle}{\langle I(t_i)I(t_i) \rangle} = \frac{(N-j)^{-1} \sum_{i=1}^{N-j} I(t_i)I(t_{i+j})}{\langle I(t)^2 \rangle},$$

where $\tau_j = t_{i+j} - t_i$.

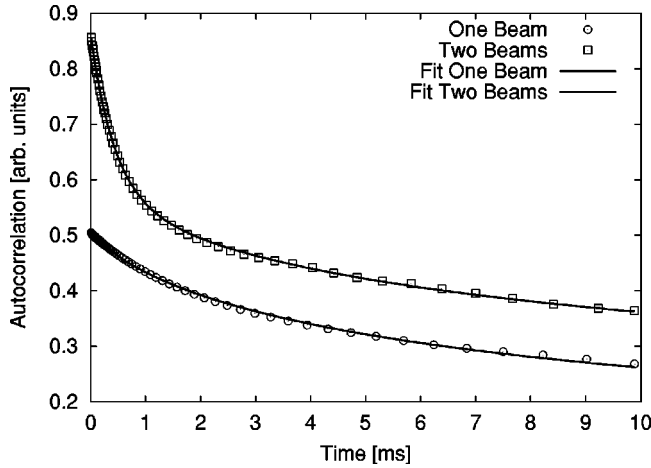


FIG. 7. Intensity-intensity autocorrelation function measured for 70-nm beads diffusing through the evanescent fringes, $C_{xz}(\tau)$ (\square), and in the evanescent field without the fringes, $C_z(\tau)$ (\circ). Continuous lines correspond to the best fit with Eq. (3).

In Fig. 7, we give an example of autocorrelation function characterizing the Brownian motion of a free 70-nm-radius bead in the buffer solution. The intensity-intensity autocorrelation functions correspond, respectively, to the bead motion through the evanescent fringes [$C_{xz}(\tau)$] and to the motion in the evanescent field without fringes [$C_z(\tau)$] (Fig. 7).

Both $C_z(\tau)$ and $C_x(\tau) = C_{xz}(\tau) - C_z(\tau)$ can be calculated analytically:

$$C_x(\tau) \propto e^{-Dq^2\tau}, \quad (3a)$$

$$C_z(\tau) \propto \sqrt{\frac{D\tau}{\pi\zeta^2}} + \frac{1 - \frac{2D\tau}{\zeta^2}}{2} e^{D\tau/\zeta^2} \operatorname{erfc}\left(\sqrt{\frac{D\tau}{\zeta^2}}\right). \quad (3b)$$

With independent measurements of $C_x(\tau)$ and $C_z(\tau)$, the diffusion coefficient D and the penetration depth ζ are measured independently. D is obtained directly from Eq. (3a) and ζ can be estimated by fitting the curve C_z with Eq. (3b).

Experimentally, we find $\zeta = 85 \pm 10$ nm and a diffusion coefficient consistent with the viscosity of pure water.

Figure 8 shows the autocorrelation function for kinesin-coated beads moving on a microtubule in 50- μ M ATP buffer. The curves correspond to a total observation time of 21 s. Because of the limited processivity of kinesin (a few micrometers), autocorrelation functions are limited in time and the curve is not significant much further than a few seconds.

The autocorrelation function can be described as an exponentially damped cosine [21]:

$$\phi(\tau) \propto \cos(qv_0\tau) e^{-q^2\tilde{D}\tau} + C, \quad (4)$$

where C is a constant value and v_0 is the mean velocity of the bead, which was measured (Fig. 8) as 120 nm s^{-1} (three times smaller than the speed measured in the same experimental environment, but at 1-mM ATP concentration) [11]. The exponential envelope of the autocorrelation function corresponds to velocity dispersion and can be classically de-

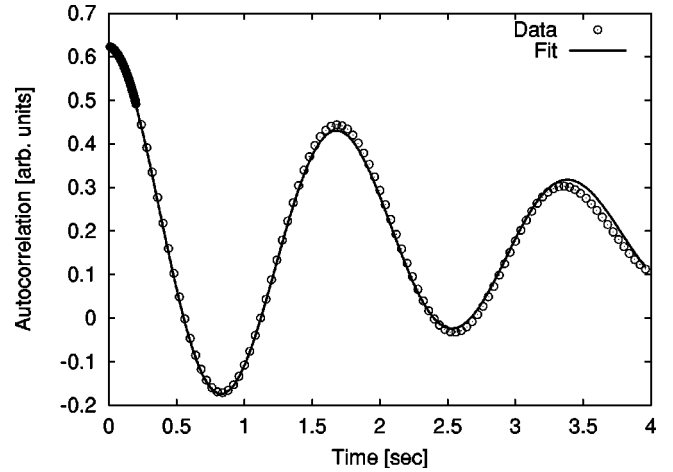


FIG. 8. Long-time autocorrelation function. Oscillations are due to the light modulation when the bead passes from a maximum to a minimum of the fringe pattern; their frequency is proportional to the kinesin speed as shown in Eq. (4). The cosinelike function is exponentially damped because of the motor randomness. The continuous line is the best fit between data and Eq. (4).

scribed by the effective diffusion coefficient \tilde{D} . This point was detailed for molecular motors by Svoboda *et al.* [22]. A randomness parameter r was introduced as

$$r = \lim_{t \rightarrow \infty} \frac{\langle x^2(t) \rangle - \langle x(t) \rangle^2}{\ell \langle x(t) \rangle} = \frac{2\tilde{D}}{\ell v_0},$$

where ℓ is the kinesin step.

For a Poisson enzyme, $r = 1$ and $r = 1/2$ for a one-step and a two-step sequential process, respectively. The continuous line in Fig. 8 represents the best fit between experimental data (\circ) and Eq. (4). The best agreement was obtained for $\tilde{D} = 315 \text{ nm}^2 \text{ s}^{-1}$, which corresponds to $r = 0.66 \pm 0.07$. This value is consistent with earlier experiments [22], although somewhat large compared to more recent ones [5]. Under the same experimental conditions, but in different runs, we observe a dispersion of r of ± 0.25 . This dispersion is probably due to the short run lengths, which do not exceed a few seconds. This value is consistent with numerical simulations which give a variation of r of ± 0.15 for runs of 250 s [21].

Figure 9 shows the autocorrelation function measured for beads interacting with a microtubule in the presence of ATP at short time: $\tau \ll 1/\tilde{D}q^2$ and $\tau \ll 1/v_0q$. We observe that the experimental data (\circ) depart significantly from $\phi(\tau)$, as expected for small values of τ from Eq. (4) (dashed line in Fig. 9).

The origin of this mismatch can be understood by comparing with the autocorrelation functions measured, respectively, for a bead attached to the microtubule in the absence of ATP (\square) and for a single bead stuck on the coverslip (\triangle).

The correlation function of the last curve (\triangle) is dominated by the intrinsic noise of the experimental setup, which includes the motion of the free beads diffusing through the fringes. We observe that the amplitude is weak compared to

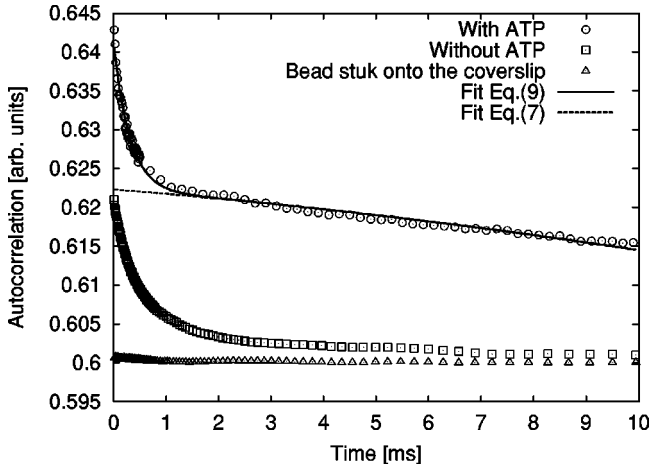


FIG. 9. Short-time autocorrelation function measured for a bead walking through the interference pattern (\circ) and for a bead attached to the microtubule in the absence of ATP (\square). The third curve (\triangle) corresponds to a single bead stuck on the coverslip. The continuous line is the best fit between data with ATP and Eq. (5).

the curves with molecular motors (\circ and \square). Furthermore, we do not observe an appreciable difference between the curve with ATP and the one without ATP. Therefore, the experiments suggest that the submillisecond behavior is neither due to the motion of the free beads nor to the kinesin motion.

The Brownian motion of the bead, tethered to the microtubule via the kinesin, probably gives rise to the short-time correlation decay. This decay contains information about the motor-bead linkage: if the linkage is weak and no external forces are applied, the bead wiggles as a Brownian particle attached to a spring in a viscous medium. In this framework, we expect Eq. (4) to be modified in the following way:

$$\phi(\tau) = \left\{ \exp \left[-\frac{q^2 k_B T}{\kappa} (1 - e^{-(\kappa/\xi)\tau}) \right] \right\} \times \cos(qv_0\tau) e^{-q^2 \bar{D}\tau} + C, \quad (5)$$

where κ is the bead-motor linkage elastic modulus, ξ is the friction and R is the bead radius. The fit yields $\kappa = 0.1 \pm 0.02$ pN/nm and $\xi = (2.8 \pm 0.8) \times 10^{-5}$ pN s/nm.

Current estimates of the kinesin-microtubule stiffness, under load, range between 0.3–1 pN [6,23]. The value mea-

sured in the absence of external load is rather lower, which is probably due to the highly nonlinear bead-kinesin-microtubule compliance found by Svoboda *et al.* [24]. At zero force, we might explore the entropic elasticity of the microtubule-kinesin-bead linkage. Applying a force of a few piconewtons would increase the stiffness by a factor of 5 and allow a 40 μ s bead response time. The value of the friction coefficient is high, but comparable with the values found by Nishiyama *et al.* [6]. Indeed they find a response time $\tau = 72 \mu$ s and $\kappa \approx 0.3$ pN/nm, which yield $\xi = \kappa\tau \approx 2.1 \times 10^{-5}$ pN s/nm. An interpretation in terms of viscous drag, using Stoke's law, yields a viscosity 30 times greater than that of water. Such a high value cannot be accounted for by standard corrections due to the proximity of a substrate [25]. It might be due to high friction on the thick casein passivation layer or by nonspecific absorption on the microtubules.

IV. CONCLUSION

In this paper, we illustrate, with the example of the kinesin molecular motor, the potential of an experiment based on the use of interference total internal reflection. We show that in a single run one can extract not less than five characteristics of the motor and bead-motor linkage: average velocity, dispersion (hence randomness), step size, bead-motor elastic modulus and bead friction coefficient. The step is identified in the absence of any external force and in physiological ATP concentration: the obtained value, 8 nm, is consistent with values obtained in low ATP concentration and with piconewton external forces. The detection speed allows, in principle, for microsecond (or better) resolution, but for now the bead response time limits the resolution to 200 μ s. Reducing friction and stiffening the bead-motor elastic linkage should allow microsecond time resolution. Such a resolution is needed for a complete analysis of the motor stepping dynamics.

ACKNOWLEDGMENTS

We warmly thank F. Nédélec for the gift of the expression vector of kinesin from *E. Coli*, M. Schliwa for providing kinesins from *Neurospora Crassa*, P. Chaikin for help with the initial setup, and A. Roux and B. Goud for their essential and continuous help in molecular biology.

-
- [1] K. Svoboda, C.F. Schmidt, B.J. Schnapp, and S.M. Block, Nature (London) **365**, 721 (1993).
 - [2] J.T. Finer, R.M. Simmons, and J.A. Spudich, Nature (London) **368**, 113 (1994).
 - [3] R. Merkel, P. Nassoy, A. Leung, K. Ritchie, and E. Evans, Nature (London) **397**, 50 (1999).
 - [4] E.-L. Florin, V.T. Moy, and H.E. Gaub, Science **264**, 415 (1994).
 - [5] K. Visscher, M.J. Schnitzer, and S.M. Block, Nature (London) **400**, 184 (1999).
 - [6] M. Nishiyama, E. Muto, Y. Inoue, T. Yanagida, and H. Higuchi, Nat. Cell Biol. **3**, 425 (2001).
 - [7] Y. Inoue, A.H. Iwane, T. Miyai, E. Muto, and T. Yanagida, Biophys. J. **81**, 2838 (2001).
 - [8] G. Steinberg and M. Schliwa, J. Biol. Chem. **271**, 7516 (1996).
 - [9] D. Raucher and M.P. Sheetz, Biophys. J. **77**, 1992 (1999).
 - [10] H. Higuchi, E. Muto, Y. Inoue, and T. Yanagida, Proc. Natl. Acad. Sci. U.S.A. **94**, 4395 (1997).
 - [11] M.J. Schnitzer and S.M. Block, Nature (London) **388**, 386 (1997).

- [12] J.R. Abney, B.A. Scalettar, and N.L. Thompson, *Biophys. J.* **61**, 542 (1992).
- [13] K.B. Migler, H. Herve, and L. Leger, *Phys. Rev. Lett.* **70**, 287 (1993).
- [14] M. Born and E. Wolf, *Principles of Optics* (Cambridge University Press, Cambridge, 1999).
- [15] B. Goldberg, *J. Opt. Soc. Am.* **43**, 1221 (1953).
- [16] J. Dai and M.P. Sheetz, *Methods Cell Biol.* **55**, 157 (1998).
- [17] T. Surrey, M.B. Elowitz, P.E. Wolf, F. Yang, F. Nédélec, K. Shokat, and S. Leibler, *Proc. Natl. Acad. Sci. U.S.A.* **95**, 4293 (1998).
- [18] W. Hua, E.C. Young, M.L. Fleming, and J. Gelles, *Nature* (London) **388**, 390 (1997).
- [19] Preliminary experiments on wild type kinesin give the usual velocity values.
- [20] F. Nédélec (private communication).
- [21] M. Badoual, G. Cappello, and J. Prost (unpublished).
- [22] K. Svoboda, P.P. Mitra, and S.M. Block, *Proc. Natl. Acad. Sci. U.S.A.* **91**, 11782 (1994).
- [23] S. Jeney, E.L. Florin, and J.K. Hörber, *Methods Mol. Biol.* **164**, 91 (2001).
- [24] K. Svoboda and S.M. Block, *Cell* **77**, 773 (1994).
- [25] L.P. Faucheux and A.J. Libchaber, *Phys. Rev. E* **49**, 5158 (1994).